



Investigation on Physical Properties of Ring-Type Wigglers Combined with a Miniaturized Column†

VINAYA KUMAR JHA¹, DAE-WOOK KIM², SEUNGJOON AHN², TAE-SIK OH², HO SEOB KIM² and YOUNG CHUL KIM^{3,*}

¹Department of Physics and Nanoscience, Sun Moon University, 100 Kalsanri, Tangjeong-myun, Asan-si, Chungnam 336-708, Republic of Korea

²Department of Information Display, Sun Moon University, 100 Kalsanri, Tangjeong-myun, Asan-si, Chungnam 336-708, Republic of Korea

³Department of Optometry, Eulji University, 553, Sanseong-daero, Sujeong-gu, Seongnam-si, Gyeonggi-do 461-713, Republic of Korea

*Corresponding author: Tel: +82 31 740 7201; E-mail: yckim@eulji.ac.kr

AJC-13318

Characteristics of ring-type electrostatic wigglers for free electron radiation have been analyzed using a 3D simulation tool. The distribution of electric potential, electric field strength affects the motion of electron beam within a wiggler system and they are determined by the bias voltage and wiggler design. In this report, these factors are carefully investigated for a few ring-type wigglers and the results offer a criterion for optimization of ring type wigglers attached to a miniaturized electron column.

Key Words: Microcolumn, Wiggler, Electromagnetic radiation, THz wave, Simulation.

INTRODUCTION

Wide spectral range of electromagnetic wave has been extensively studied since electromagnetic waves have been closely related with our lives and various types of electromagnetic sources have been developed and used for tremendous purposes. However, considering the practical electromagnetic sources, there is a gap corresponding to THz region which attracts much interest recently because of its potential applications in near future, for example in bio-technological area and they are still under developing stage¹⁻⁴.

Free electron radiation module is one of the most appropriate tools for generating waves with wide spectral range including THz wave. A high energy electron beam freely moving through a wiggler or an undulator will generate wave and the period of wiggler determines the wavelength of the spectrum⁵. A wiggler is introduced to supply transversely accelerating motion to electrons such that electron beam oscillates periodically while it passes through the wiggler, which generates electromagnetic wave⁶⁻⁹. Therefore, a wiggler is an important component in free electron radiation and magnetic wigglers have been generally adopted for deflecting charged particles. After electrostatic wiggler was proposed by Motz¹⁰, several related works have been reported¹¹⁻¹⁴. Recently, a ring-type electrostatic wiggler was proposed replacing the conventionally adopted planar type wiggler in order to obtain highly symmetric oscillation than the planar type⁹. In this work, we analyzed some characteristics of a ring-type wiggler such

as the variation of electric potential and field depending on the wiggler structure. The factors affecting the optimized wiggler structure will be discussed.

EXPERIMENTAL

Modeling: Though a ring-type wiggler has been suggested since the electron beam (e-beam) shows overall deviation from the optical axis⁹ in a conventional planar type wiggler, detailed characteristics of the ring-type wiggler were not studied enough. For the future application as a THz wave source based on the free electron radiation and an electrostatic wiggler system, we have designed a few ring-type wiggler systems with different inner diameter and studied their properties using a simulation tool. The basic structure of a ring-type wiggler is a stack of repeated layers of conducting electrodes and insulating layers. In this work, the thickness of a conducting layer is 4 μm and that of an insulating layer is 1 μm . For the real fabrication, a SOI wafer with 4 μm -thick highly doped active layer and 1 μm -thick oxide layer can be used. Taking a conducting and an insulating layer as a basic unit, the whole wiggler system is designed to be composed of total 20 basic units as shown in Fig. 1.

We have investigated some physical properties by varying the inner diameter of the wiggler from 20, 50 and 100 μm . Fig. 2 shows the whole free electron radiation module composed of an electron source and a ring-type wiggler. The electron source is composed of an electron emitter and three

†Presented to the 6th China-Korea International Conference on Multi-functional Materials and Application, 22-24 November 2012, Daejeon, Korea

electrostatic electrodes. The first one (S1) is to extract electrons from the emitter, the second one (S2) is an accelerating electrode and the third one (S3) is a limiting aperture to eliminate the highly diverging electrons. We applied a negative bias to the emitter (for example, $V_{\text{Tip}} = -300$ V in this case) and S1 and S3 are grounded. Since the field emitted electron beam passing through the limiting aperture is a diverging beam and it may hit the electrodes after entering the wiggler. Therefore, we applied a negative bias voltage to S2 electrode ($V_{S2} = -240$ V in this case) in order to make the e-beam nearly parallel to the optical axis or slightly converging.

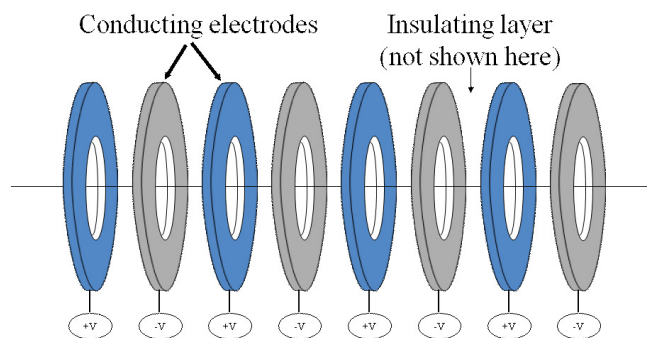


Fig. 1. Schematic structure of a ring-type wiggler

For the generation of radiation, the electrons need to transversely oscillate while passing through the wiggler region. In order to motivate this oscillation, normally alternating bias potentials are applied to the wiggler electrodes as shown in Fig. 1. In this work, we set this bias potential as ± 50 V or sometimes higher voltage for the comparison.

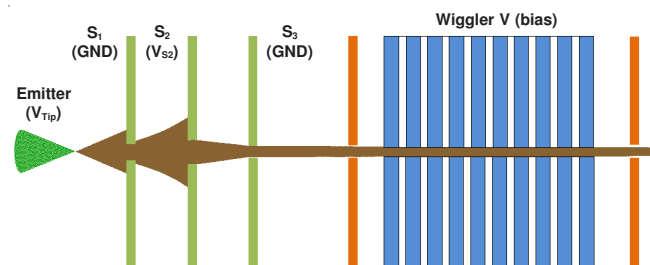


Fig. 2. Schematic diagram of the free electron radiation module composed of an electron source and a wiggler

RESULTS AND DISCUSSION

Fig. 3(a) and (b) present the electric potential distribution estimated on the plane containing X-axis (or r-axis) when the inner diameter is $20 \mu\text{m}$. The bias voltage was ± 50 V for both (a) and (b). In this figure, the origin of z-axis was selected as the tip-end of the electron emitter.

As expected by the wiggler design and the bias voltage, electric potential shows basically periodic feature. When the diameter is larger than $50 \mu\text{m}$, the difference of (a) and (b) is the overall distortion of potential due to the electric field leakage at both edges of the wiggler. One of the most important points is that the potential height seems to be dependent on the distance from the circumference of the wiggler electrode hole to the interesting point, not on the radius (r) itself. In other words, it mainly depends on $R-r$, where R is the inner radius

of the wiggler electrode and r is the distance from the optical axis to the interesting point (Fig. 3). The oscillation of potential is crucial for the electromagnetic wave radiation since it will result in oscillating electric field and finally transverse oscillating motion of electrons. In this figure, we can observe the clear oscillating feature when r is large ($R-r$ is small) but this feature becomes weak with decreasing r (increasing $R-r$).

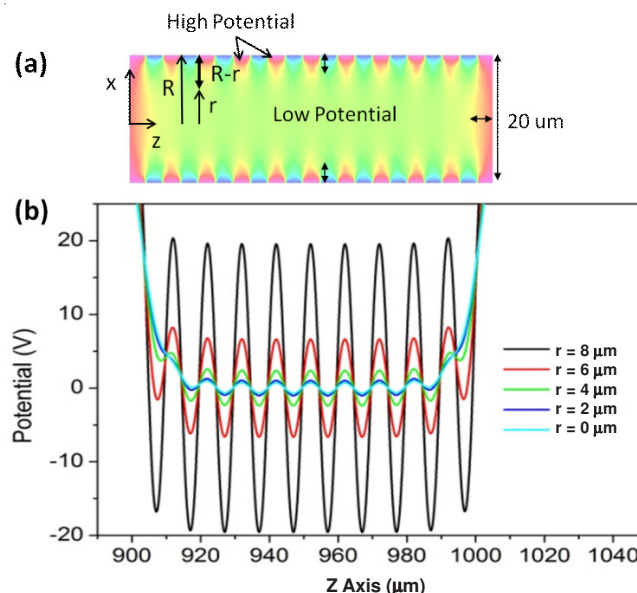


Fig. 3. Distribution of electric potential inside the wiggler region on the plane containing x-axis (or r-axis) when the inner diameter is $20 \mu\text{m}$

To make it clear, we have plotted the potential variation depending on $R-r$ estimated at various bias potential, from 20 V to 100 V. Fig. 4 shows the potential variation across the radial direction at the middle electrode for two ring-type wigglers with $20 \mu\text{m}$ and $50 \mu\text{m}$ inner diameters. The solid and open symbols represent the data from $20 \mu\text{m}$ and $50 \mu\text{m}$ wigglers, respectively. As shown in this figure, potential value decreases monotonically with $R-r$ and becomes lower than 5 V when $R-r$ is greater than around $7 \mu\text{m}$. Comparing these graphs, it is difficult to find any critical difference except the small differences in potential value when $R-r$ is smaller than ~ 5 or $6 \mu\text{m}$. The potential is high enough when $R-r$ is smaller than a certain value, d , where d is to be determined by some parameters such as bias potential, wiggler diameter and the e-beam diameter.

The variation of electric field strength across the wiggler region when ± 50 V bias voltage is applied to the wiggler electrodes is presented in Fig. 5. In this figure, the left and right graph represent the electric field strength for $20 \mu\text{m}$ and $50 \mu\text{m}$ wiggler, respectively. As in the case of potential, electric field strength is decreasing with $R-r$ and the typical strength is $\sim 10^7$ V/m when $R-r$ is small.

All the above argument indicates that there must be a criterion in designing a ring-type wiggler. There is a sort of effective region inside the wiggler in which the electric field strength is strong enough to force the e-beam oscillate to generate electromagnetic radiation.

This effective region looks like a disk with a hole at its center. The outer diameter of this disk is R and inner diameter

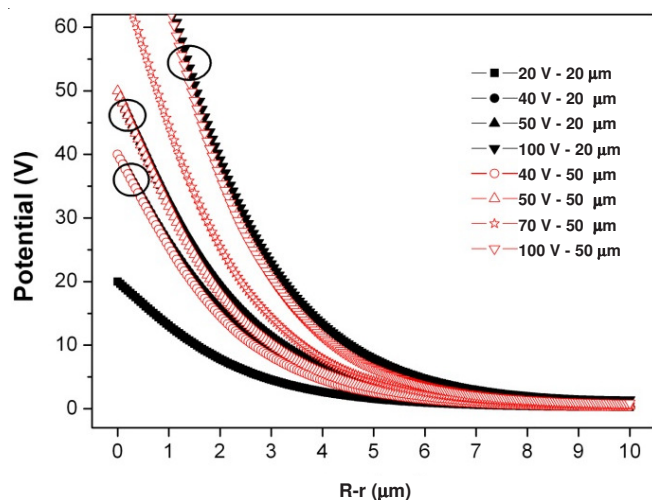


Fig. 4. Potential variation along the radial direction at the middle electrode when the wiggler inner diameter is 20 μm and 50 μm

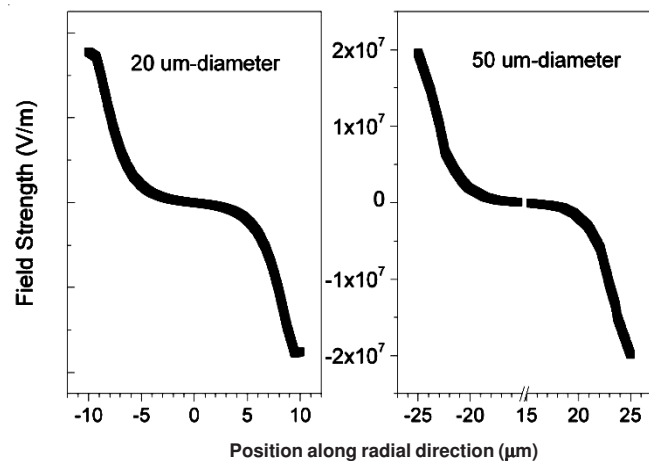


Fig. 5. Variation of electric field strength along the radial direction at the middle electrode for both 20 μm and 50 μm wiggler

is $R-d$. As the effective region is confined within a region, $R > r > R-d$, e-beam entering the wiggler is to pass through this region. Thus one of the design targets is to make the effective region large and another is to keep the e-beam passing through this region.

It seems to be advantageous to apply higher bias potential considering the magnitude of potential and its decreasing tendency (Fig. 4) (decreases slowly when the bias voltage is higher like 100 V). However, the situation is a little bit complicated. If we set the bias voltage too high, the beam bend so much toward the optical axis even at the entrance region of the wiggler, which means that the beam approaches near the optical axis after short travelling along the wiggler and does not feel strong oscillating field any more.

If we increase wiggler diameter R , for example $R = 100 \mu\text{m}$, we can get larger effective area. However, the e-beam

passing the wiggler hardly showed oscillating motion when simulation was done for 100 μm diameter wiggler. This is because we assumed the diameter of limiting aperture as 50 μm through in this work. So, in order to increase wiggler diameter, we must modify the electron beam source part since the diameter of e-beam entering the wiggler is normally limited by the limiting aperture shown in Fig. 2.

Therefore, we need to consider several parameters such as e-beam diameter, wiggler diameter and the bias voltage, etc. In order to increase d , higher bias voltage is required. At the same time, wiggler diameter is to be increased to some extent and e-beam diameter correspondingly.

Conclusion

We have investigated characteristics of a free electron radiation module based on an electron source and ring-type electrostatic wiggler systems using a 3D simulation tool. Electron trajectory and oscillatory motion inside a wiggler system is directly affected by the variations of potential and electric field strength, which have been carefully investigated for a few selected ring-type wigglers. The results indicate that we need to consider a specific region inside a wiggler in which field is strong enough to result in the transverse oscillatory motion of electron beam. In order to design an optimized wiggler, some physical parameters are to be considered simultaneously combined with the electron source structure.

ACKNOWLEDGEMENTS

This work was supported by Eulji University in 2012 and the IT R & D program of MKE/KEIT. [10039226, Development of actinic EUV mask inspection tool and multiple electron beam wafer inspection technology].

REFERENCES

1. S. Kumar, B.S. Williams, S. Kohen, Q. Hu and J.L. Reno, *Appl. Phys. Lett.*, **84**, 2494 (2004).
2. M. Nagel, P.H. Bolivar, M. Brucherseifer, H. Kurz, A. Bosserhoff and R. Buttner, *Appl. Phys. Lett.*, **80**, 154 (2002).
3. K. Kawase, J. Shikata and H. Ito, *J. Phys. D: Appl. Phys.*, **35**, R1 (2002).
4. G. Gallot, S.P. Jamison, R.W. McGowan and D. Grischkowsky, *J. Opt. Soc. Am. B*, **17**, 851 (2000).
5. S.J. Smith and E.M. Purcell, *Phys. Rev.*, **92**, 1069 (1953).
6. H. Yiping and Chen Deming, *Int. J. Infrared Millimeter Waves*, **11**, 73 (1990).
7. A. Murai, K. Mima, S. Kuruma, N. Ohigashi, Y. Tunawaki, K. Imasaki, S. Nakai and C. Yamanaka, *Nucl. Inst. Meth. A*, **331**, 680 (1993).
8. V.A. Papadichev, *Nucl. Inst. Meth. A*, **393**, 403 (1997).
9. Y.C. Kim, S.J. Ahn, H.-S. Kim, D.-W. Kim and S.J. Ahn, *Nucl. Inst. Meth. A*, **654**, 427 (2011).
10. H. Motz, *J. Appl. Phys.*, **22**, 527 (1951).
11. G. Bekefi and R.E. Shefer, *J. Appl. Phys.*, **50**, 5158 (1979).
12. A. Anselmo and J.A. Nation, *IEEE Trans. Nucl. Sci.*, **32**, 3494 (1985).
13. A. Anselmo and J.A. Nation, *Phys. Fluids*, **31**, 2037 (1988).
14. S. Riyopoulos, *Phys. Rev.*, **E56**, 4710 (1997).